DUCTILITY OF REINFORCED MASONRY SHEAR WALLS AND IMPACT OF INCOMPLETE GROUTING

M.T.Shedid[1], A.A.Hamid[2], and R.G.Drysdale[3]

[1]M.A.Sc. Candidate, Dept of Civil Engineering, McMaster University, Hamilton, ON, L8S 4L7. shedidmm@mcmaster.ca

[2] Professor and Director of the Masonry Research Lab, Drexel University, Philadelphia. Also adjunct Professor and member of the Centre for Effective Design of Structures, McMaster University, hamida@mcmaster.ca

[3] Professor, Martini Mascarin and George Chair in Masonry Design and Director of the Centre for Effective Design of Structures, McMaster University, drysdale@mcmaster.ca

ABSTRACT

The possibilities of achieving a high level of energy dissipation in reinforced concrete masonry shear walls mainly by flexural yielding are examined. The experimental response of three walls, tested as the first phase of an investigation of the cyclic lateral load response of reinforced concrete masonry shear walls, is discussed. The amount of vertical reinforcement and the influence of an accidental incomplete filling of a reinforced masonry shear wall with grout are reported in this paper. The results show high ductile capability in the plastic hinge region and very little degradation of strength for cyclic loading.

KEYWORDS: walls, ductility, plastic hinging, lateral deformation

INTRODUCTION

In regions where strong earthquake ground motions are anticipated, it is generally not efficient to design shear walls to remain elastic during a severe earthquake. Therefore, inelastic deformations are expected, usually at the base of the wall, to reduce the force that the wall must be designed to resist by changing the response of the structure and by dissipating energy. The inelastic deformations can also be thought of as providing a fuse to limit forces on other structural elements [1, 2]. In shear walls, a ductile response can be achieved through the development of a flexural plastic hinge at the base that allows for significant dissipation of energy.

In previous and current editions of the National Building Code of Canada [3], reinforced masonry shear wall construction has been considered to be relatively a brittle form of construction compared to similar reinforced concrete construction. “Seismic design of masonry structures commonly involves a high level of conservatism, which is mostly attributed to masonry’s poor performance during past earthquakes” [4]. Lack of comprehensive data on plastic hinging and energy dissipation of reinforced masonry has also contributed to creating this situation. However, results of many studies have consistently revealed that masonry, when properly proportioned, detailed, and constructed, provides adequate safety against seismic forces [3, 4].

This paper presents experimental data on behaviour of three reinforced masonry shear walls.

EXPERIMENTAL PROGRAM

The experimental data presented is the first phase of an investigation of the response of flexural concrete masonry shear walls. The variable studied is the effect of the amount of vertical reinforcement in the wall. As the result of incomplete filling of one wall with grout, the influence of this construction problem is an accidental but very interesting additional variable included in this phase of testing. The walls were tested under lateral cyclic reversed displacement patterns simulating earthquake excitation. Details of the three test walls and the test data are presented below.

DETAILS OF TEST SPECIMEN

The walls had an aspect ratio of two (3.6 m high and 1.8 m long) to allow plastic hinges to form, and were fully grouted using hollow 20 cm concrete blocks. The vertical and horizontal reinforcement were uniformly distributed across the wall panel. The horizontal reinforcement consisted of No. 10 bars with the 350 mm long 180-degree hairpin shaped hook around the outmost vertical reinforcement located 100 mm from the ends of the wall as shown in Figure 1(a). The amounts of reinforcement shown in Table 1 were selected to ensure that yielding of tension reinforcement would occur based on an assumed maximum strain in masonry of ε_m = 0.002. A capacity design approach using actual yield strength of steel was implemented to avoid shear failure.

As shown in Table 1, Walls 1 and 2 were reinforced identically with No. 25 vertical bars in each cell and No. 10 bars acting as shear reinforcement in each course of masonry. Wall 2 was required as a duplication of Wall 1 because areas with empty or partially grout filled cells were discovered during the wall test. Wall 3 had slightly more than half as much vertical reinforcement as Walls 1 and 2. The horizontal shear reinforcement started in the first course with a spacing of 2 courses. The vertical reinforcement was accurately located and anchored into a 600 mm x 500 mm base as shown in Figure 1(b). The bars were detailed to have sufficient length not to require splices. This avoided complications in interpreting data with flexural response affected by development length and extra reinforcement. The concrete blocks were placed by an experienced mason using S type mortar. For courses containing horizontal reinforcement, the webs of the blocks were cut to half block height and knocked out (see Figure 1(c)), to create space for this reinforcement and to permit it to be fully encased in grout.

Fine grout commercially available from a ready-mix company was pumped into the full 3.6 m wall height. Problems with the pumping equipment and with achieving a sufficiently fluid grout resulted in major ungrouted areas of Wall 1 which were undetected until partway through the test. Wall 3 was found to have some minor areas with incomplete grout filling. These were filled prior to testing by grout injection using nonshrink ready mix grout pumped through 25 mm diameter holes. No unfilled grout spaces were detected in Wall 2.

Table 1 – Details of wall reinforcement

Wall	Vertical reinforcement		Horizontal reinforcement	
	$\rho_v = A_s / t L$	No. and size	$\rho_h = A_v / t s$	Size & spacing
1 & 2	1.31 %	9 25M	0.26 %	10M@200mm
3	0.73 %	5 25M	0.13 %	10M@400mm

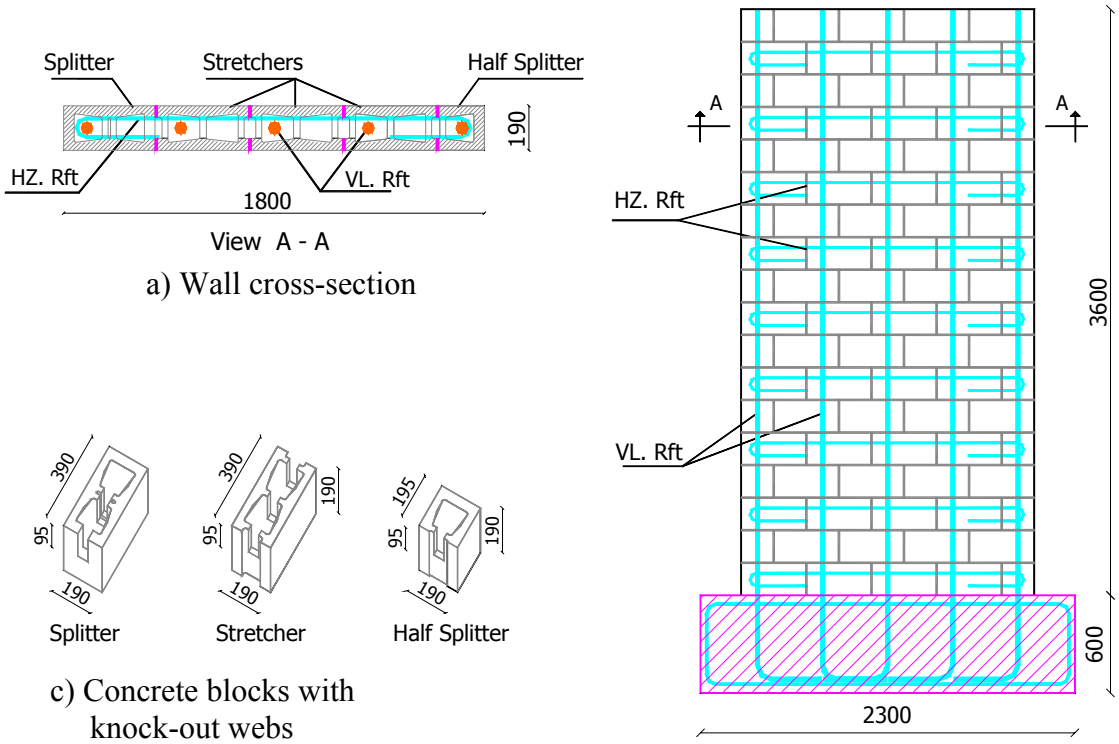

Figure 1 – General Specimen Details

TESTING AND INSTUMENTATION

The test setup in Figure 2 shows the concrete base of the test wall prestressed onto a large concrete slab which had been prestressed onto the strong floor of the laboratory. At the top of the wall, the vertical reinforcement extended through and was welded to a U-shaped built-up steel loading beam. It was designed to simulate the transmission of the earthquake load to the shear wall by applying uniform lateral load along the top of the wall instead of as a single concentrated load. The horizontal load was supplied though a 1400 kN MTS hydraulic actuator aligned with the top of the masonry wall. Rollers were attached to braces which prevented out-of-plane displacement at the top of the wall. Displacement control was used to provide the cyclic loading.

During testing, loads, deflections and strains were monitored using a data acquisition system for 41 readings at 7 seconds intervals. Twenty-one wire potentiometers were used to monitor vertical, horizontal and diagonal deformation on the masonry as well as base slip and wall uplift. The configuration of deformations measurements created a strain rosette required to distinguish between shear and flexural deformation. As shown in Figure 3(a), to measure lateral deflection relative to the base, eight potentiometers were attached at different heights to a truss supported on a steel beam cantilevered from the reinforced concrete base of each specimen. The distribution of axial deformation at the wall ends and the uplift from the concrete base were measured using 14 wire potentiometers installed vertically along the wall height. These were also used to calculate the curvature of the wall. One potentiometer was mounted horizontally on the concrete base to measure any horizontal slip between the wall and its concrete base. All strings

connected to the potentiometers were attached to a steel bracket at the base level to avoid losing all readings when spalling of masonry due to toe crushing occurred.

In addition to the above external instrumentation, 10 electrical strain gauges were applied to the vertical reinforcing steel as shown in Figure 3(b), prior to wall construction. These were placed within the most highly stressed region to monitor the first yield as well as the extent of yielding over the height of the wall and the penetration of bar yielding inside the concrete base.

The cyclic loading sequence adopted in the first two walls tested consisted of two full cycles at each displacement which was increased in 2 mm increments. The sequence was repeated until the specimen lost 50% of its maximum load resistance which was adopted as the failure criteria in this study. The yield deflection, Δ_y, for each specimen was defined as the deflection of the wall at first yielding of the outermost vertical bar as recorded by the electrical strain gauge at the interface between the wall and the reinforced concrete base. After establishing that significant ductility and large displacement were to be expected as characteristic behaviour from the response of Walls 1 and 3, Wall 2 was tested with increments of yield displacement after first yield.

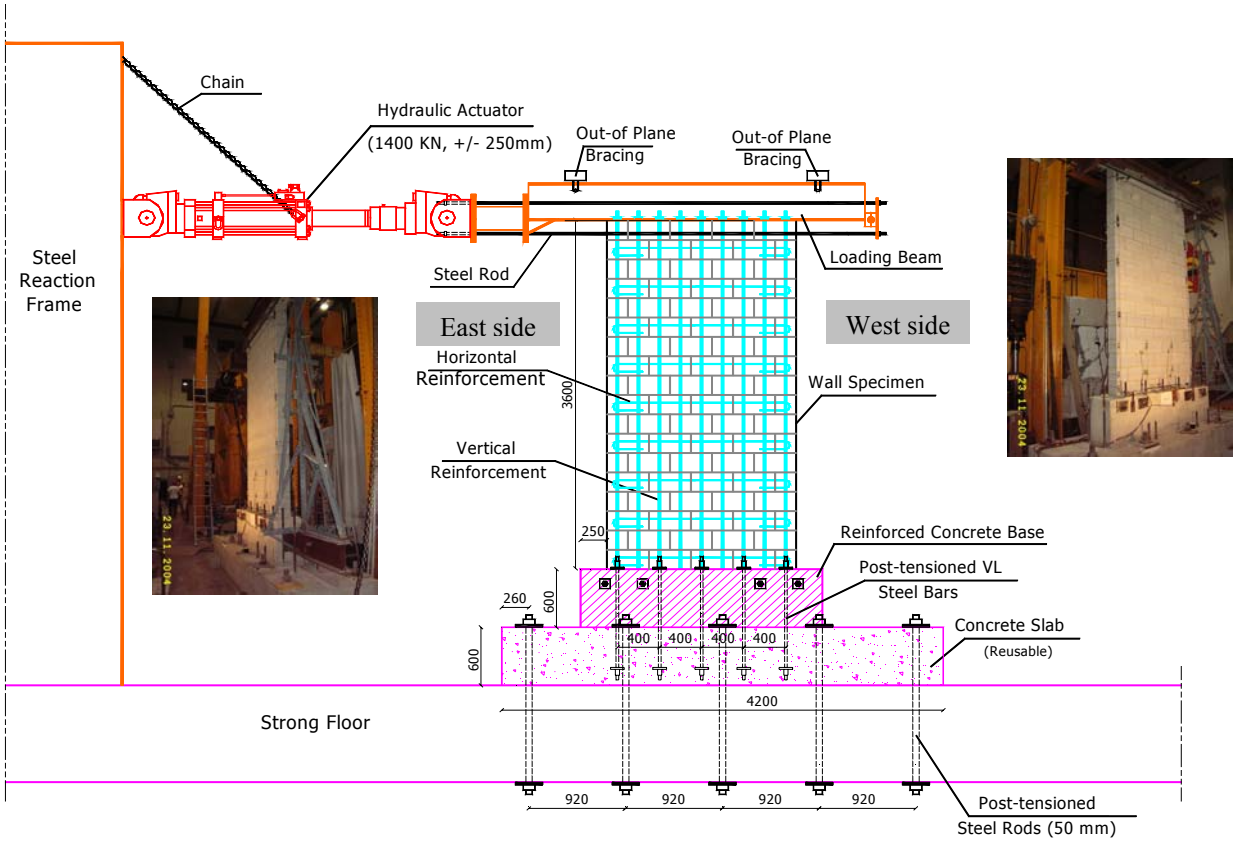

Figure 2 – Test Setup

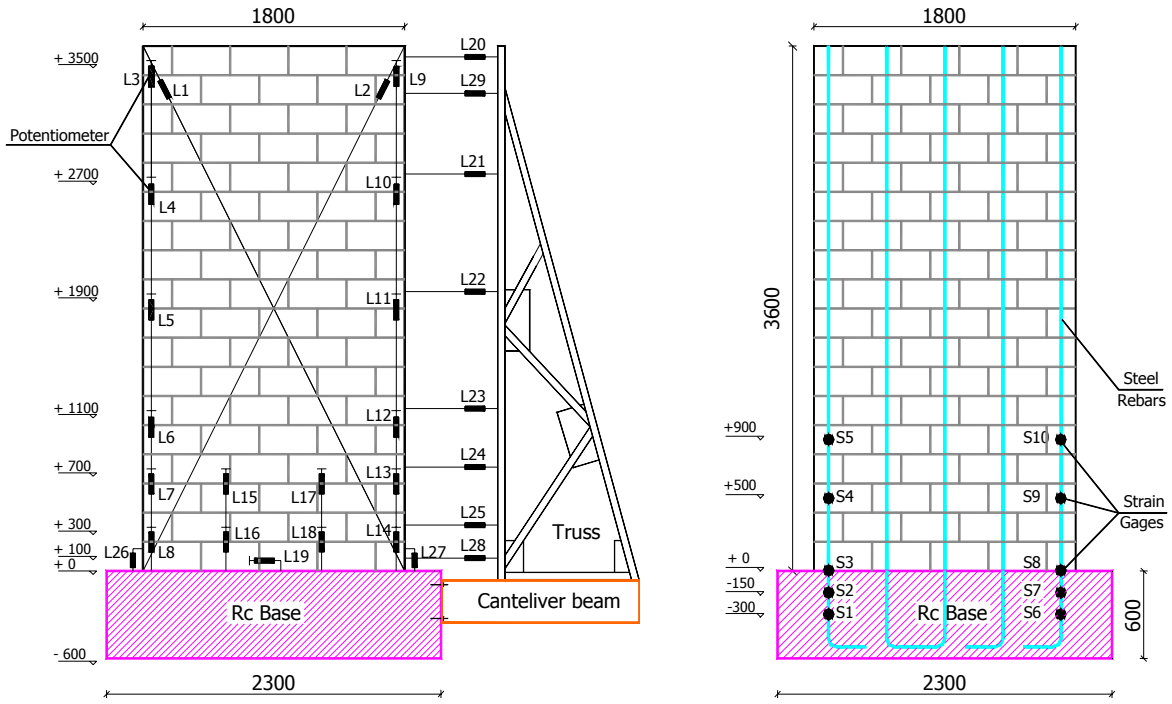

a) Displacement potentiometers locations

b) Strain gauges locations

Figure 3 – Instrumentation

TEST RESULTS

Behaviour of all walls was dominated by flexural response which was clear from the amount of horizontal cracking along the bed joints. Clearly visible but minor diagonal stepped cracks formed just before yielding of the outermost vertical bar and were observed over the height of the wall after maximum load was reached. All walls displayed reasonable symmetry in push and pull cycles until toe crushing occurred in both sides. After failure occurred in both toes, the walls lost a significant amount of their out-of-plane stiffness.

During the initial phase of testing Wall 1, symmetry of hysteresis curves for cyclic loading (see Figure 4(a)) and response reasonably close to predicted values masked the presence of ungrouted zones. It was only after toe crushing that some indications of presence of ungrouted areas were observed. A vertical crack, at 200 mm from the east wall edge, extended from the second course up to the tenth course (see Figure 5(a)). Also, very wide horizontal cracks were observed prior to maximum load as shown in Figure 5(b). Examination of the 200 mm long column at the East end of the wall during the test revealed that this region was entirely empty of grout leaving the reinforcing bar unsupported and unbonded to the wall (see insert in Figure 5 (c)). Increased wall deflection with increased lateral load extended past yielding of the outermost reinforcing bar. The sudden drop in the load at 24 mm displacement during the pull cycle (see Figure 4(b)) corresponds to maximum load and beginning of complete separation of the 200 mm long column containing the empty end cell. At this point, the east end was in compression. Due to a slight misalignment between Wall 1 and the actuator, the out-of-plane bracing system was not strong enough to resist the misaligned load in the push mode. Therefore, at large displacements, Wall 1

was subjected to incremental reversed pull cycles with only a partial push cycle. The gradual decrease in load with increasing displacement up to 50 mm is shown in Figure 4(b).

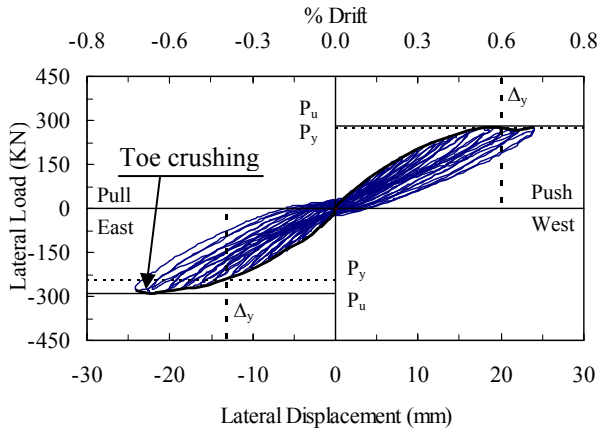

a) Hysteresis curves for Wall 1 prior to toe crushing

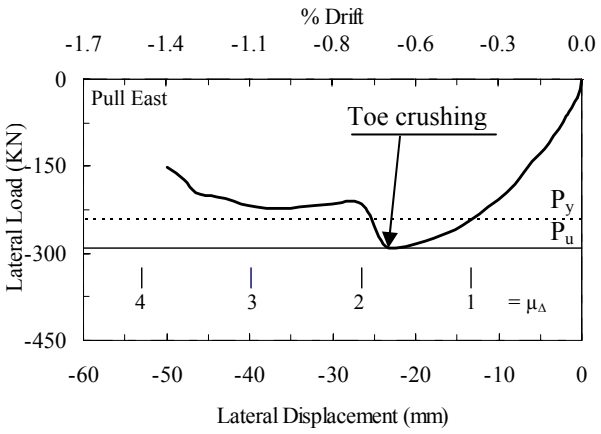

b) Envelope of load-displacement for Wall 1 in pull direction

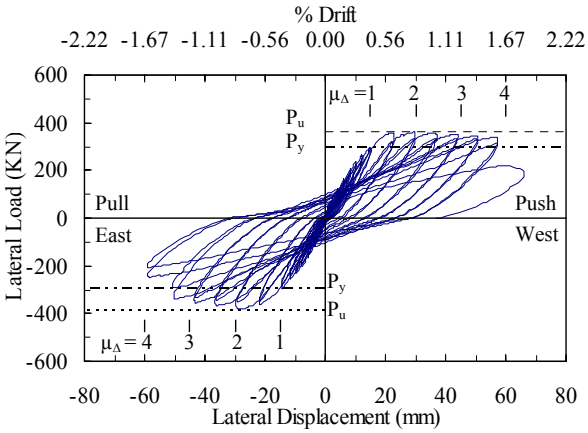

c) Hysteresis curves for Wall 2

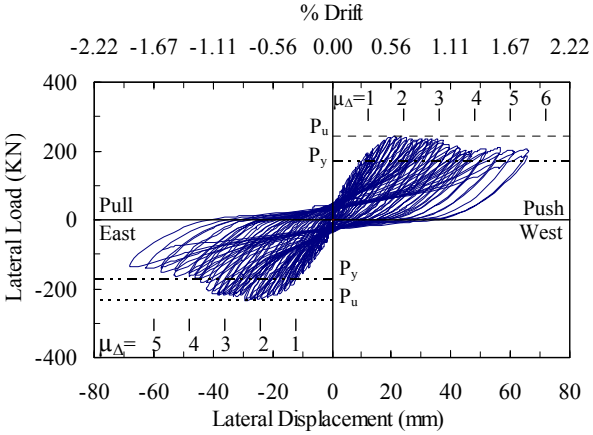

d) Hysteresis curves for Wall 3

Figure 4 – Cyclic Load-Displacement Response of Test Walls

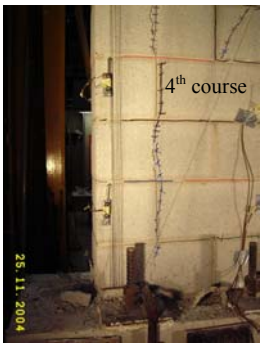

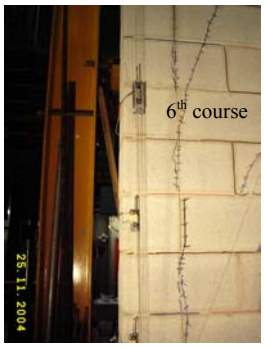

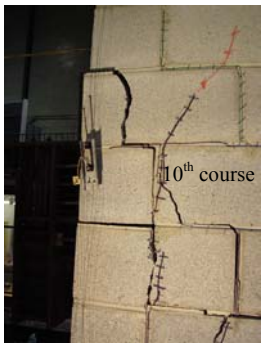

a) Vertical cracking at East end of Wall 1 **b)Horizontal cracking in Wall 1**

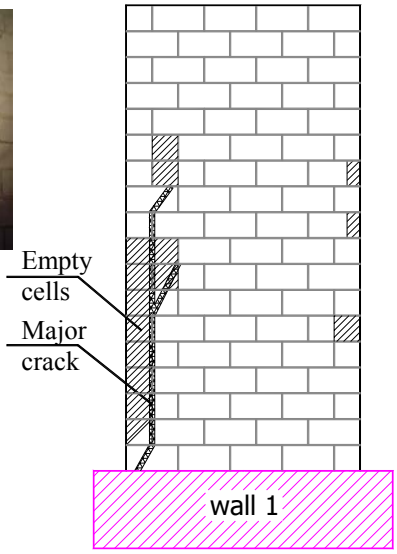

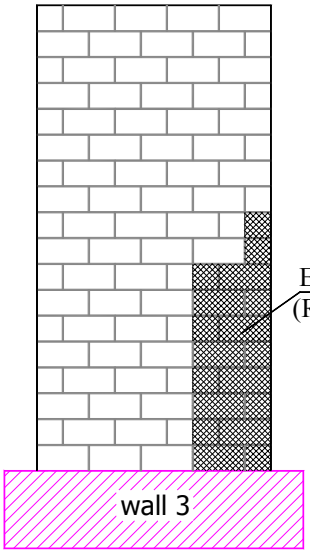

c) Empty cells in Wall 1 **d) Empty cells in Wall 3**

Figure 5 –Cracking and Unfilled Cell Information

LOAD DISPLACEMENT RESPONSE

The hysteresis curves plotted in Figure 4(a) show symmetric behaviour of Wall 1 before toe crushing in spite of the empty column of grout located in a critical zone. The sudden drop in the load displacement curve shown in Figure 4(b) during the pull part of the loading cycles identifies the stage when the 200 mm column containing the ungrouted end cell separated from the wall. Following eventual spalling of this region, buckling of the unsupported end bar under compression could be seen clearly. The fact that this bar significantly contributed in the lateral resistance of the wall can be seen from the long horizontal plateau of the load-displacement envelope shown in Figure 4(b) for the pull direction. From strain measured on the outermost bars, the yield displacement in the push direction was much greater than in the pull direction as the elongation in the unbonded bar was accumulated over the unbonded length of the bar. The data showed that it yielded at the base only after reaching the maximum lateral push load.

The similar crack patterns for all walls indicated flexural response. Wall 3, having a critical part of its west side regrouted (see Figure 5(d)), displayed symmetry in the pull and push directions

(see Figure 4(d)). Large crack widths were detected between the wall and the base and extended along the whole length of the wall. Vertical cracks started to appear in the East and West toes at displacements significantly beyond those corresponding to the maximum lateral load. Wall 3 did not experience severe degradation in strength for push loading unlike what occurred in the pull direction (see Figure 4(d)). During the push cycle causing first tension yield in the east bar, displacement was not stopped quickly enough to avoid some yielding deformation. As a result, the yield displacement in the pull direction was slightly higher. Buckling of the end reinforcing bars was observed after spalling of the masonry during the test and, at the beginning of the 75 mm push cycle, the test was terminated as the outermost East reinforcing bar broke and the wall lost strength.

As can be seen in Figure 4 (c), the pattern of loading adopted for Wall 2 differed from the previous two walls in the size of displacement increments applied after first yield. The strains recorded in the two outermost end reinforcing bars were monitored during the test and once one of these bars reached the yield strain, the loading was stopped and the lateral force was reversed to avoid having plastic deformation in the bar. As a result, unlike Wall 3, the yield displacements for Wall 2 were the same for the pull and push directions. This facilitated interpretation and tracking of the stresses and forces in the reinforcing bars. Wall 2 experienced more degradation of strength in the pull direction than in push direction (see Figure 4(c)). More extensive masonry spalling and buckling of the end reinforcing bar in the pull direction were observed to coincide with significantly decreased resistance. At the end of the test, the outermost two east bars buckled in the pull direction whereas only the outermost west bar was observed to buckle.

General wall behaviour is summarised in Table 2, where the V values are the maximum lateral force recorded in the push and pull directions and the Δ values are the corresponding recorded lateral displacements. The displacements, $\Delta_{0.75v}$ and $\Delta_{0.50v}$, are defined as the points at which the lateral wall strength had degraded to 75% and 50%, respectively, of maximum lateral load V. The predicted flexural strength based on a maximum masonry compressive strain of 0.002 is defined as $F_{n,}$ and Δ_n is the predicted maximum lateral displacement based on plastic hinge height equal to half the wall length and only flexural deformations [1, 5, 6]. The displacements at first yield are defined as Δ_y. F_y and V_y indicate predicted and recorded yield load. It should be noted that although the masonry code [1] does not include untied compressive steel in strength calculations, compressive reinforcement does contribute to capacity and ductility.

Table 2 – Summary of Test Results

	Predicted without comp. steel (With comp. steel)				**Measured for Push direction (Pull direction)**					
	Δ_y	F_y	Δ_n	F_n	Δ_y	V_y	Δ	V	$\Delta_{0.75v}$	$\Delta_{0.50v}$
W1					--- (13)	--- (231)	18 (22)	274 (291)	--- (40)	--- (50)
W2	8.65 (8.54)	300 (303)	12.6 (13.84)	332 (370)	15 (15)	296 (292)	30 (30)	360 (380)	57 (50)	65 (58)
W3	8.10 (8.03)	192 (195)	16.1 (17.8)	238 (253)	10.6 (14)	174 (190)	23 (29)	242 (235)	--- (46)	--- (68)
units	mm	KN	mm	KN	mm	KN	mm	KN	mm	mm

Although, the measured curvature at the base of the wall calculated from the two strain gauges located at the interface between the wall and the base was almost the same as the predicted value at first yield, the yield deflection predicted using elastic loading theory was significantly less than the measured yield deflection. In fact, in-plane lateral deflection is comprised of sliding, flexural and shear displacement. Although there is no direct method to distinguish between flexural and shear components of deflection, they have been evaluated using the model by Massone and Wallace [7] using elongation measurements of the X diagonally oriented string potentiometers and the vertical wire potentiometers over the full height of the wall. As shown in Figure 6(a) for Wall 2, very good correlation was found between the measured and the calculated deflections using the selected model. Similar agreement was found for Wall 3. A decrease in the percent of flexural displacement with increase of total lateral deflection can be seen as presented in Figure 6(b). The flexural deflection at first yield was found to account for only 72% which can partially explain the significant difference between the predicted and measured deflections. Use of flexural deflection calculations seems to be inadequate as the shear deformations are significant. [Note: It is essential to include vertical displacement effects as simple use of diagonal displacement measurements result in significant overestimates of deflection due to shear deformations.]

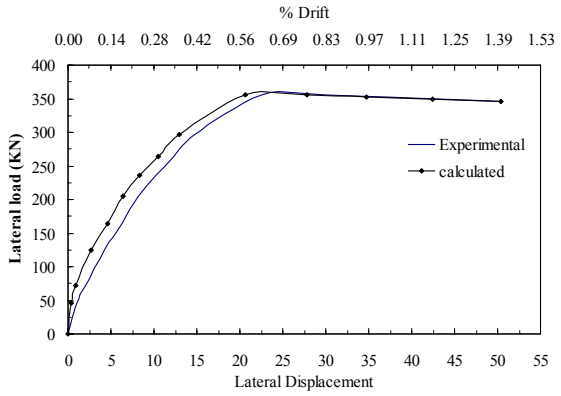

a) Experimental Vs calculated lateral deformation for Wall 2

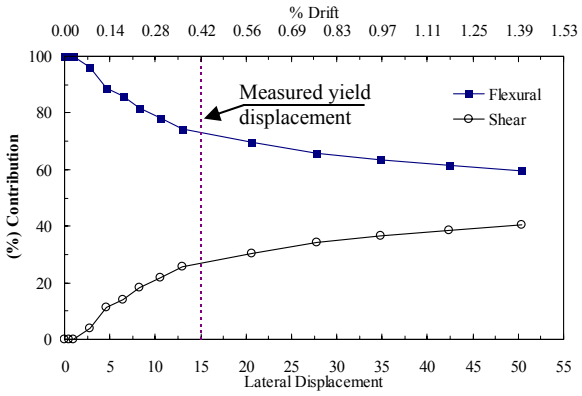

b) % of Flexural and shear deformation in total lateral displacement

Figure 6 – Flexural and Shear Deformations for Wall 2

The curvatures calculated from vertical displacement measurements for Walls 2 and 3 are shown in Figure 7. As can be seen, the yield region reached a height of between 800 and 900 mm.

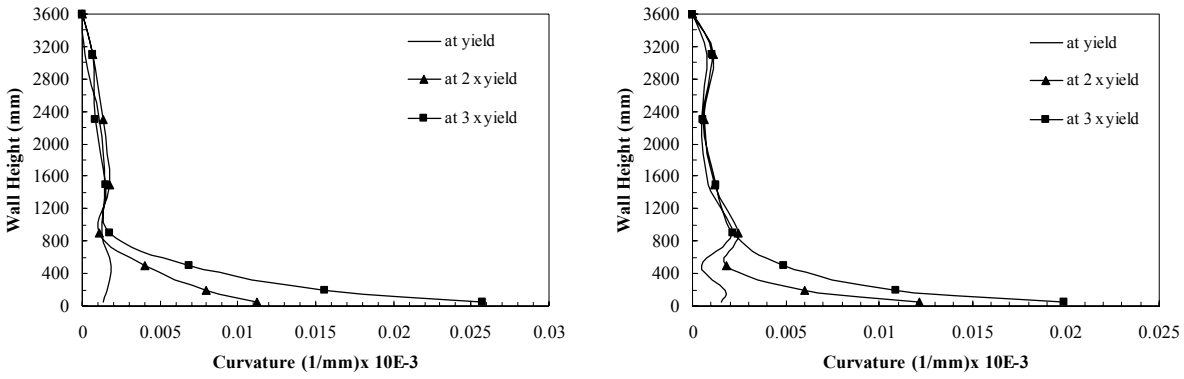

a) Wall 2 b) Wall 3

Figure 7 – Curvature Distribution along the Wall Height

AUXILARY TESTS

Masonry compression strength f'_m= 15.2 MPa was determined by testing of 4 block high grout filled masonry prisms. Samples taken from the No. 25 reinforcing bar had an average yield stress of 506 MPa. Block molded grout prisms (95 x 95 x 190 mm) gave an average compressive strength of 37.8 MPa.

DISCUSSION AND OBSERVATION

- The presence of ungrouted zones in Walls 1 and 3 illustrate the difficulty in achieving complete filling. Mortar droppings and the practice of filling these walls in lifts led to this problem as the grout tended to set up and bridge over open spaces between cycles of grouting. The wall that was continuously grouted over the full 3.6m height was completely filled with grout. The presence of a major flaw in Wall 1 did not have a large influence on energy dissipation and resulted in only about a 25% reduction in capacity.
- Standard methods of calculating deflection based on flexure underestimate both deflection and ductility. For Wall 2, which was heavily reinforced, the deflection of maximum load was 2 times the yield deflection and this increased to 3.3 times with only 25% degradation in strength. In contrast, the calculated value was 1.45 for maximum load and post-peak response could not be determined. For the more lightly reinforced Wall 3, the predicted and measured displacement ductilities at maximum load were fairly similar but again calculation could not include the benefit of permitting some degradation of strength. In terms of ability to dissipate energy, it can be seen that setting ultimate displacement beyond maximum load justifies much greater reduction in equivalent static loading than predicted by standard calculations.
- Buckling of untied compression reinforcement did not occur until after significant strength degradation was observed. Therefore, ignoring the beneficial contribution of this reinforcement to strength and ductility is questioned.
- Accurate prediction of cyclic behaviour requires careful tracking of stress in reinforcement to account for the effect of the successive compressive and tensile yielding in the bar.

ACKNOWLEDGEMENTS

This research was conducted as a part of the mandate of the McMaster University Centre for Effective Design of Structures funded through the Ontario Research and Development Challenge Fund (ORDCF). Provision of mason time by Ontario Masonry Contractors' Association and Canada Masonry Design Centre is appreciated. The supply of concrete blocks and grout by Boehmer Block Ltd is gratefully acknowledged.

REFERENCES

1. J. H. Thomsen and J. Wallace. "Displacement-Based Design of slender reinforced Concrete Structural Walls- Experimental Verification." J. Struct. ASCE, Vol. 130, No.7, April, 2004.
2. R. Tremblay, P. Leger, and J. Tu., "Inelastic Seismic Response of Concrete Shear Walls Considering P-delta Effects." Canadian Journal of Civil Engineering. Vol. 28, 2001.
3. NBCC. National Building Code of Canada. Institute for Research in Construction, National Research Council of Canada, Ottawa, 2005.
4. Haluk Scuoglu and Hugh D. Mcniven. "Seismic Shear Capacity of Reinforced Masonry Piers." J. Struct. Div., ASCE, Vol. 117, No.7, July, 1991.
5. T. Paulay and M. J. N. Priestley (1992). "Seismic Design of Reinforced Concrete and Masonry Buildings". John Wiley and Sons, New York, N.Y.
6. Robert G. Drysdale, Ahmad A. Hamid, and Lawrie R. Baker. "Masonry Structures- Behaviour and Design" second edition, The Masonry Society, Boulder, Colorado, 1999.
7. Leonardo M. Massone and John W. Wallace. "Load-Deformation responses of Slender Reinforced Concrete walls". ACI Structural Journal, Vol. 101, No.1, January, 2004.
8. Canadian Standards Association, "Masonry Design of Buildings". CSA, S304.1-04, CSA Mississauga, Ontario, 2004.